PERGAMON

International Journal of Solids and Structures 38 (2001) 7691–7701

INTERNATIONAL JOURNAL OF SOLIDS and STRUCTURES

www.elsevier.com/locate/ijsolstr

Influence of roughness on characteristics of tight interference fit of a shaft and a hub

G.M. Yang [a], J.C. Coquille [b], J.F. Fontaine [c,*], M. Lambertin [d]

[a] *Centre de Ressources Technologique, route de Monéteau, 89 000 Auxerre, France*
[b] *Ecole Nationale d'Enseignement Supérieur Agricole de Dijon, 21000 Quetigny, France*
[c] *Laboratoire de Recherche en Mécanique et Acoustique, IUT route des plaines de l'Yonne, 89 000 Auxerre, France*
[d] *Laboratoire Bourguignon des Matériaux et Procédés, ENSAM, CER Cluny, 71250, France*

Received 2 August 1999

Abstract

Tight interference fits are very widely applied in industry, because of their simple manufacturing process. But, in all proposed models for determining their characteristics, one supposes that the contact interfaces are perfect. This is not the case in reality. The objectives of this study are to analyse the contact surfaces behaviour under the effect of the assembly pressure. We show for a given surface texture typology that the roughness has a noticeable influence on the fit strength. Our process uses an experimental approach correlated with numerical modelling of the assembly. The aim is to justify a tightening definition based on the maximum matter concept and to introduce, for this particular case, a prediction of loss due to the deformation of the surface asperities. © 2001 Elsevier Science Ltd. All rights reserved.

Keywords: Tight interference fit; Assembly; Contact with asperities; Finite element modelling

1. Introduction

1.1. Classical approach for modelling the tight interference fits

The tight interference fit, as a way of assembling two mechanical components, is widely applied in industry because it is efficient and, in theory, simple to implement. This technique is used either to add an interface part having good tribological properties to a structure (e.g. a fitting bearing on a gearbox casing), or to increase the strength of a high pressure enclosure. It can also be used to assemble a shaft and a hub on a large scale (e.g. transmission and breaking set of railway bogies) or for small and very accurate sizes (for example: video recorder drums). The presented study concerns the latter application.

* Corresponding author. Tel.: +33-3-8694-2619; fax: +33-3-8694-2616.
E-mail address: fontaine@alcyone.u-bourgogne.fr (J.F. Fontaine).

0020-7683/01/$ - see front matter
PII: S0020-7683(01)00035-X

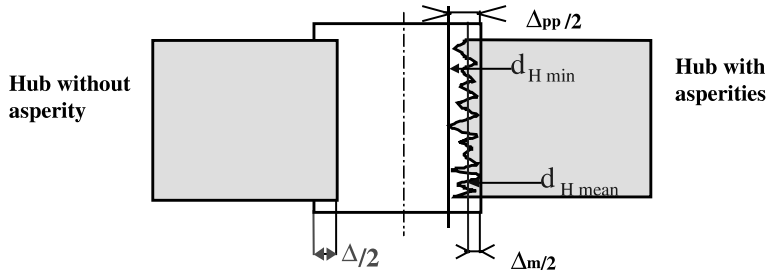

Fig. 1. Lame's model assumptions and the real behaviour.

For the calculation of the cylindrical tight fit, we use the classical approach combining the thick walled cylinder and Lamé's method of elasticity (Nicolet and Trottet, 1971). It forms the basis of the standards in most industrial countries (NF E22-621, 1980, NF E22-620, 1984).

The contact pressure can be written thus:

$$p_{\mathrm{n}} = \frac{\Delta(k^2-1)}{d[(a_{\mathrm{m}}-a_{\mathrm{a}})+k^2(a_{\mathrm{m}}+b_{\mathrm{m}})]}. \tag{1}$$

where Δ is the tightening (the difference between the axis and hub diameters), k, a geometrical factor, d, the fitting nominal diameter and a_{m}, a_{a}, b_{m}, material characteristic constants.

Note that the geometrical characteristics taken into account are only dimensional. However, the standards recommend a loss of tightening for asperity moving to take place, of course, this depends on arithmetic roughness of both contacting surfaces ($R_{\mathrm{a_s}}$, for the shaft, $R_{\mathrm{a_h}}$, for the hub)

$$L_{\Delta} = 3(R_{\mathrm{a_s}} + R_{\mathrm{a_h}}). \tag{2}$$

This expression is empirical, so our objective is to study the asperity behaviour and its contribution to the fit strength.

As Fig. 1 shows, we take into account the micro-geometry of the contacting surfaces. The tightening is not locally constant, so we have two possibilities for introducing the tightening parameter: [1]

- The mean tightening (Δ_{m}) given by the mean square method.
- The peak to peak (Δ_{pp}) given by the difference between the maximum diameter of the shaft and the minimum diameter of the hub hole.

1.2. Mechanical contact with roughness

The study of the contact between two rough surfaces is a difficult theory as well as an experimental problem.

The objective of several studies has been the analysis for of the indentation of a infinite flat rough surface by a flat smooth die: Moore (1948), Bowden and Tabor (1958), Williamson and Hunt (1972) and Childs

[1] The standards do not give more precision except for dimensional and form defect specifications based on the maximum matter criterion. However, we make an arbitrary choice here to begin the study of mean tightening definition based mathematical reasoning.

(1977) have shown that roughness persists for different experiments under high pressure greater than the elastic limit. This phenomenon is due to the hardening of the asperities and to the type of load (compression in all three directions) induced by the indentation.

Other studies concerning the laws of friction in metal forming processes present different macroscopic loads: the material is subjected to transversal tension or compression. The models are based on the slip line field method (Bay and Wahnheim, 1976; Sutcliffe, 1988), or on the finite element method (Ike and Makinouchi, 1990). They show that the boundary conditions play a predominant role in the surface roughness behaviour. A tension in the surface direction speeds up the flattening of the asperities contrary to a compression which delays it.

The tight interference fit case is different. The geometry is cylindrical and the radial and ortho-radial stresses in the hub are equal and opposite at a macroscopic scale. In a previous study, we showed the influence of form defect (Fontaine and Siala, 1998). In the case of periodic defects, on the peaks, the pressure is maximum and the ortho-radial stress minimum and vice versa on the hollows. In the case of the surface texture study where the asperity behaviour is not easily predicted, we firstly carried out an experimental study which we later correlated to a FE modelling using ABAQUS® software. The obtained experimental and numerical results show the great influence of the surface roughness. Finally, we justify that the peak to peak tightening criterion gives the best correlation with the assembly strength and we introduce a new tightening loss calculation based on numerical and experimental observations.

2. Experimental tests

The principle of the experimental tests (Yang, 1998) lies in the comparison of the extractive loads of the fitted set which have the same geometrical characteristics but different roughness values (Fig. 2). The tightening Δ_m is fixed at 25 μm for a fitting diameter equal to 16 mm. The relative tightening $\Delta/d = 1.56\%$ is consistent with the standard data.

The axes used are in fact treated steel control elements. Their cylindrical surfaces are considered perfect.

The hubs were manufactured in duralumin in accordance with the simple disk geometry given in Fig. 1 (exterior diameter = 60 mm and thickness = 10 mm). All the holes of the hubs were machined on a DNC lathe, varying the turn step to give different roughness values ($0.2\ \mu m < R_a < 6.8\ \mu m$). All of the geometrical characteristics have been measured in applying several methods to ensure the accuracy of the results. The mean tightening has been calculated by taking into account all defects. This step was very

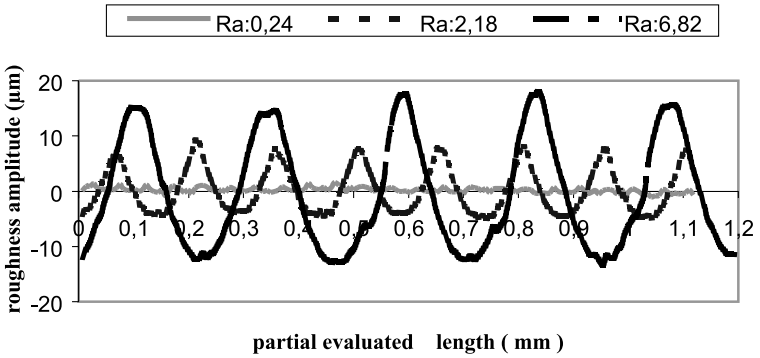

Fig. 2. Example of roughness profiles.

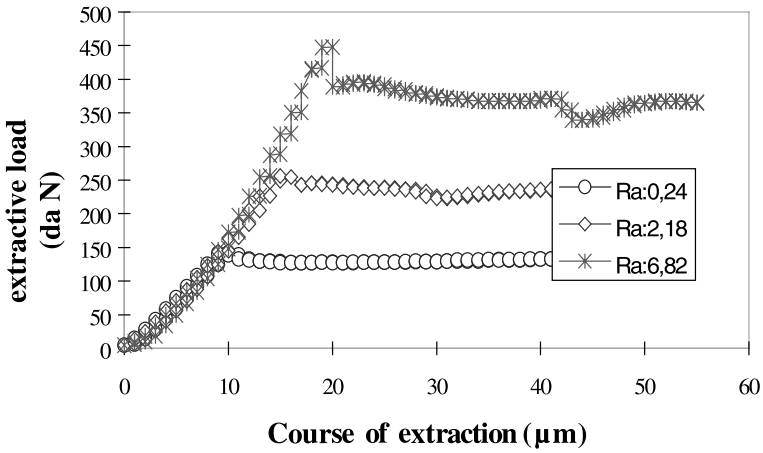

Fig. 3. Experimental extracting load for different roughness values.

delicate because each parameter (dimension, form, surface texture) was measured on a different machine. It was necessary to compile the measurements to restore the holes topography. For every class of roughness, a limited number of hubs presenting minimum defects of form and similar mean dimensions was selected and paired up with a chosen shaft. Every pair was assembled by heating the hub and free insertion of the axis.

After cooling, the strength was measured by extraction of the axis at low speed (0.5 mm/min). This characterization has the advantage of being simple to process but it is not complete: it would need to be associated with the strength of the sliding torque which is often a functional characteristic in the industrial fit cases.

We can see the evolution of the extractive load versus the relative displacement for different roughness values in Fig. 3. It is important to note that the first stage, on every curve, corresponds to the elastic rigidity of the assembly where there is no relative displacement between the contact surfaces. The roughness does not influence the latter. In a second stage, where we are concerned with the relative sliding of both parts, the load remains constant. At this stage, it is clear that the surface texture greatly influences the strength of the fit.

It is difficult to understand the asperity deformation mechanisms because it is impossible to observe the contact surface, so we have modelled the process by the finite element method.

3. Numerical modelling of the process of tight interference fit and extracting test

3.1. General assumptions

1. The axis is considered perfect before the hub bore defects Fig. 4. Table 1 shows the different characteristics of the samples.
2. The thermal dilatation step is not taken into account. It is considered not to affect the properties of materials and the interfacial micro-geometry. This can be justified by the low temperature used (200°C).
3. The roughness in the ortho-radial direction is negligible compared to that in the axial direction (see Table 2). The modelling can be effected with the assumption of the axial symmetry.
4. The behaviour is elastoplastic. The formulation is expressed in large deformations and a contact with little sliding is chosen for the fitting step.

Table 1
Comparison between the hub and the axis geometrical defects

		Number of sample		
		1	2	3
R_a, Arithmetic roughness (μm)	Hub hole	0.24	2.18	6.82
	Shaft	0.09	0.071	0.063
o, Cylindricity defect (μm)	Hub hole	9.48	8.79	8.56
	Shaft	1.72	1.87	1.04
Δ_m, Mean tightening (μm)		25.8	26.9	23

Table 2
Comparison of the surface texture characteristics in the axial and ortho-radial directions

	Number of sample		
	1	2	3
R_a axial	0.24	2.18	6.82
R_a ortho-radial	0.04	0.17	0.13
R_z axial	1.89	9.56	26.26
R_z ortho-radial		0.19	0.28

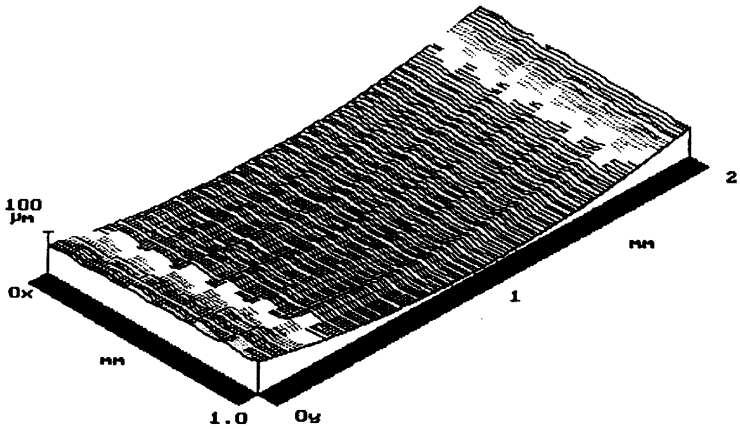

Fig. 4. Example of 3D roughness measures of the hub hole.

The coefficient of friction between steel and duralumin is taken as 0.15 by conventional value.

The mesh is made up of four-node quadrangles. This is accomplished by checking that the mesh does not influence the results while providing a good compromise vis-à-vis calculation time. A fine mesh is chosen for a zone 2 mm large near the interface. The length of element is equal to ≈20 μm. This is less than half of the smallest step of roughness than intended. So, every sample is modelled with the same mesh with respect to the following procedure:

- Choice of a characteristic sample profile: several measures are made in different surface locations. The ones with values nearest to the mean parameter values are chosen.

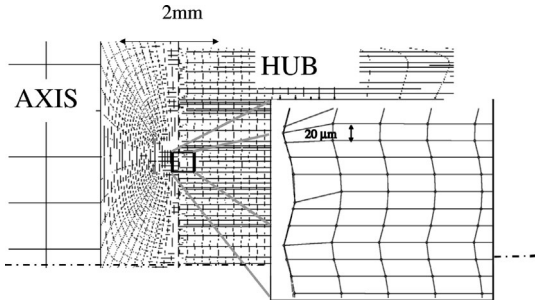

Fig. 5. Mesh of asperities with respect to peaks and hollows for $R_a = 2.4$ μm.

- Digitalization of the profile in 4000 points. The lengths are variable because of the different measuring conditions (the evaluated length depends on the filter), so the profile is completed by translation to obtain the total fitting length.
- Search of the spline curve associated to the profile points.
- Elaboration of the element with respect to the profile: it is necessary to have a node at every peak and hollow as Fig. 5 shows.

The boundary conditions are the following:

- outside surfaces are free,
- symmetry with respect to a plane perpendicular to the cylinder axis is fixed.

The tightening is applied progressively up to the value of the simulated assembly.

3.2. Extractive test simulation

The extraction step is modelled from the results of the first step with the following boundary conditions: the displacements of the axis extremity are imposed and the opposite hub face is fixed in the axial direction.

As the experimental curves present a non-monotonous response, Risk's method is used in order to make the calculations converge.

4. Results and interpretation

4.1. Extractive strength

Fig. 6 gives the evolution of the extractive force versus the axis displacement.

One can see on one hand a good correlation between the calculation results and the experimental measures. The difference can come from defects and inaccurate experimental data, such as the value of the friction coefficient. However it is less than 9% which permits us to validate our modelling. On the other hand we notice the great influence of the surface texture on the extractive strength.

The modelling permits us to bring some responses to our initial questions. The strength (R) depends on two parameters: the nominal contact pressure (p_n) and the friction coefficient (f) with:

$$R = \int_{A_n} f_{p_n} \, \mathrm{d}A_n, \tag{3}$$

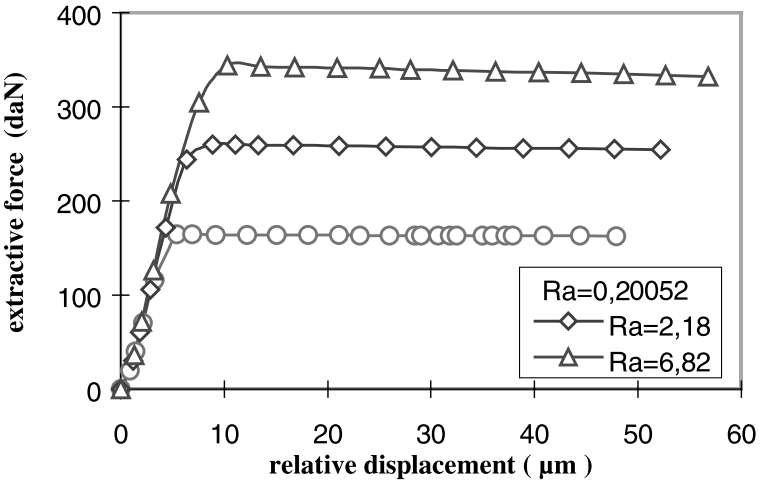

Fig. 6. Extracting force versus displacement for different roughness values.

p_n depends on the real pressure (p_r) and on the ratio between the real area (A_r) and the nominal area (A_n):

$$p_n = p_r A_r / A_n. \tag{4}$$

It is essential to study the influence of roughness on both parameters.

4.2. Contact pressure and interface stresses state

From the numerical results, it is very difficult to determine the real contact area. But the nominal pressure can be calculated from the mean contact pressure. Table 3 indicates that this grows with the roughness, and we can see that the maximum pressure increases too as a notable increase. However, the maximum level of Von Mises's stress in the hub is less than the maximum pressure. In fact it depends on the peak distribution. If the surface was perfect, the mean pressure and the maximal pressure would be equal to half of the equivalent Von Mises's stress.

In fact, the surface roughness changes the contact interface behaviour radically. Fig. 7a and b indicate the evolution of the three main stresses in a radial direction for a rough surface at a peak level and for a perfect surface. In the case of a perfect surface, the elastic limit is reached more quickly because of the state of radial compression ($\sigma_1 < 0$) and ortho-radial tension ($\sigma_2 > 0$) whereas in the case of a rough surface, there is a compressive stress in the three directions ($\sigma_1 < 0$, $\sigma_2 < 0$ and $\sigma_3 < 0$). This state is not systematic,

Table 3
Mean pressure, maximum pressure and maximum Von Mises's stress versus the roughness

Arithmetic roughness R_a (µm)	Mean pressure p_n (MPa)	Maximum pressure (MPa)	Maximum Von Mises's stress in the hub (MPa)
0.24	70.56	260	411
2.18	111.2	425	487
6.82	149.1	654	505

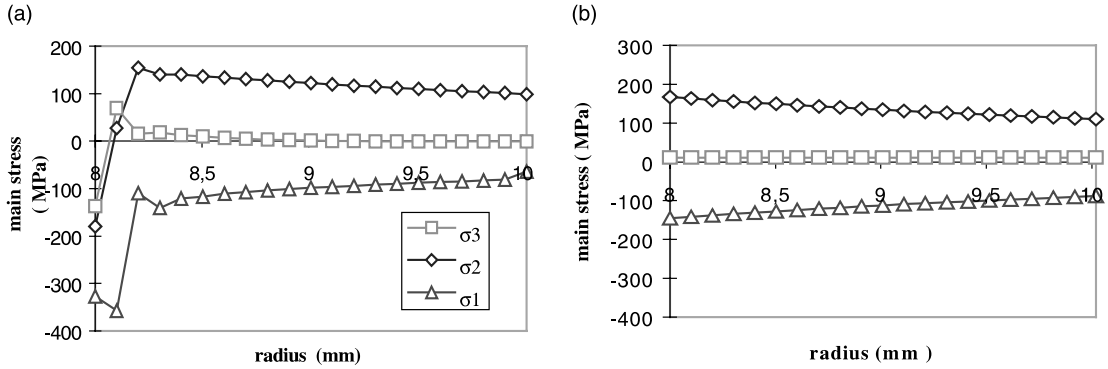

Fig. 7. Example of the evolution of the main stresses in the hub near the interface in the radial direction at a peak level. Comparison with perfect theoretical case.

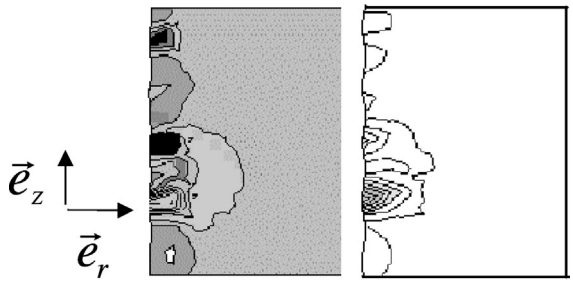

Fig. 8. Stresses field near the interface (in grey compressive stresses in white tensile stresses) to left radial stresses to right ortho-radial stress.

but due to the roughness distribution which is not perfectly periodic and depends on the relative heights of the peaks and of their neighbours.

Fig. 8 indicates the radial and ortho-radial stresses field. The radial stresses are negative and the ortho-radial stresses are globally positive but near certain peaks they are negative (something which delays the change in plasticity).

A further study will examine the interaction between the surface asperities. Finally, we observe that the stresses in the hub are not maximum stresses at the interface but are so under the peaks as shown in Fig. 9.

One can conclude that in spite of the favourable stress conditions to crush the asperities, they have a tendency to persist even under great pressure.

4.3. Friction coefficient

It is very difficult to predict the evolution of coefficient of friction. If it is presumed that the thermal step has not modified the material properties, its evolution would come from variation of surface texture. Table 4 indicates that the different surface texture parameters do not change very much. These parameters are calculated from the numerical simulations. We notice that the roughness decreases just a little, which means that the asperities persist. The total height of the profile (P_t) is smaller after assembly so the lone peaks are

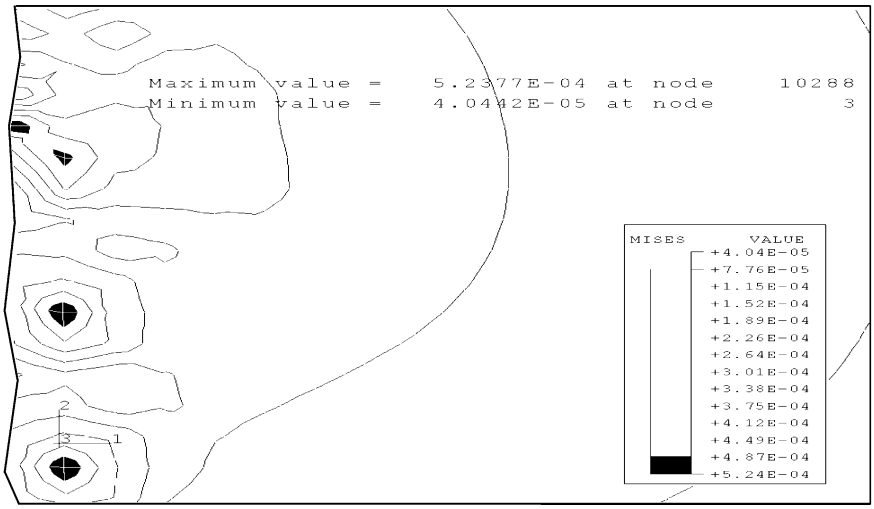

Fig. 9. Von Mises's stress distribution for $R_a = 2.18$ μm: areas with plasticity deformation are represented in black.

Table 4
Comparison of surface texture parameters before (b) and after assembly (a)

Group		Hub					Axis				
		R	R_x	W	W_t	P_t	R	R_x	W	W_t	P_t
1	b	0.6	1.2	0.8	1.9	2.0	–	–	–	–	–
	a	0.5	1.1	0.8	1.2	1.2	0.1	0.2			0.3
2	b	9.6	12.6	2.8	3.5	13.6	–	–	–	–	–
	a	9.2	11.2	2.8	3.4	11.8	0.2	0.3		0.4	0.4
3	b	24.1	26.0	2.4	2.7	26.9	–	–	–	–	–
	a	22.9	24.3	2.4	2.3	24.4	0.2	0.3		0.5	0.5

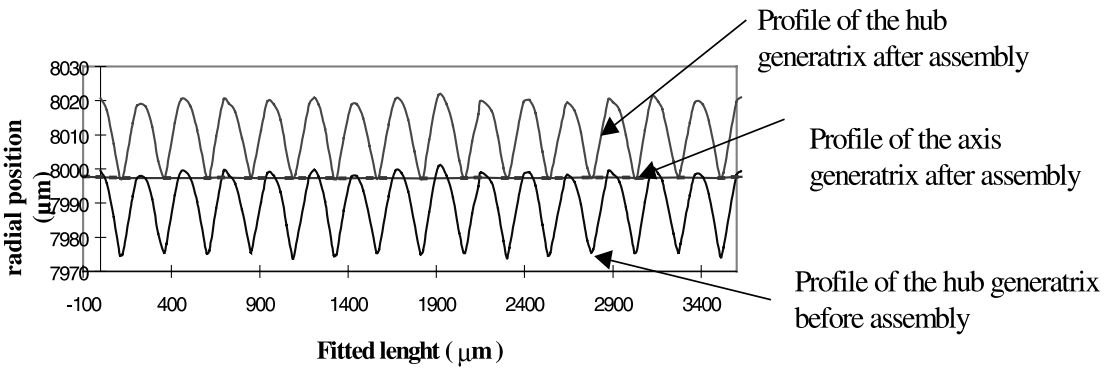

Fig. 10. Profile of the hub before and after assembly.

very deformed until the contact involves all the peaks (see Fig. 10). The axis, considered perfect at the beginning, presents a low roughness level due to the great difference in hardness between both materials.

We can estimate that the coefficient of friction does not change in the case of the given problem.

5. A best definition of the tightening

From the elements given previously, it can be concluded that if the mean tightening parameter (using the mean squares method) is used to define the characteristic parameter of the fit, the surface texture will notably influence the assembly strength. Since the surface roughness persists after assembly, it could be said that they contribute to the tightening. This is the reason why we have introduced the second definition of the tightening (Δ_{pp}) consistent with the maximum matter concept (see Fig. 1).

The peak to peak tightening (Δ_{pp}) is defined by:

$$\Delta_{pp} = d_{s\,max} - d_{h\,min} = \Delta_m + 2R_{pb}, \tag{5}$$

where $d_{s\,max}$ is the maximum diameter of the shaft, $d_{h\,min}$ is minimum diameter of the hub hole, Δ_m is mean tightening, R_{pb} is maximum height of the hub peaks of the outside cylinder.

Concerning the tightening loss, it can be limited to the plastification of the isolated peaks. It can be directly eliminated at the time of the measurement if the "motifs" method is used (Boulanger, 1992) or it can be determined by subtracting the double distance between the highest peak and the mean peak line of the hub profile:

$$\Delta_{pp\,corrected} = \Delta_{pp} - 2(R_{ph} - R_{pmh})$$

Table 5 shows the comparison for the precedent example between the extractive force measured and calculated from the standard model (I) using the proposed tightening with the different corrections. One can see that the proposed tightening loss is better than the one given in the standards.

To verify the validity of our approach, we have simulated three fits each with an identical peak to peak tightening and different roughness values as shown in Fig. 11. The extracting forces given in Fig. 12 are

Table 5
Comparison between the measured and calculated extractive forces: (I) without tightening loss, (II) suggested loss $L_\Delta = 2(R_{ph} - R_{pmh})$, (III) standard loss: $L_\Delta = 3(R_{a_s} + R_{a_h})$

R_a	Measured force	Δ_{pp} (I)	Calculated force	$\Delta_{pp\,corrected}$ (II)	Calculated force	$\Delta_{pp\,corrected}$ (III)	Calculated force
0.24	1570	28.6	1867	27.46	1793	28.12	1836
2.18	2690	44.7	2918	42.1	2749	40.34	2634
6.82	3720	60	3917	55.4	3617	46.36	3027

Coefficient of correlation between the calculated forces and the measured forces: 0.99995 (I), 0.99999 (II) and 0.9856 (III).

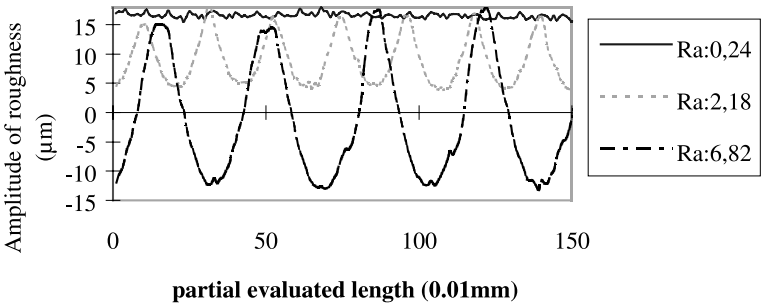

Fig. 11. Three hub profiles presenting the same peak to peak tightening.

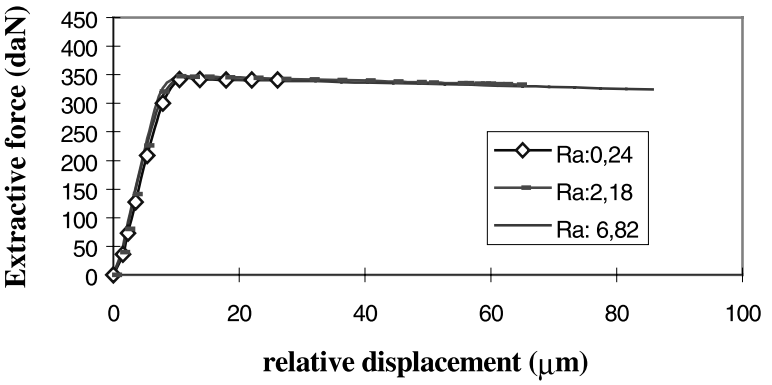

Fig. 12. Extractive force obtained by numerical simulation for three fits having different arithmetic roughness values and an identical peak to peak tightening.

identical for the three roughness values therefore demonstrating the validity of the peak to peak tightening definition.

6. Conclusions

Based on the results obtained through a series of experimental tests and associated numerical simulations, this paper shows the asperities behaviour for the cylindrical tightening fit of an axis and a hub. These analyses confirm that the asperities play an important and positive role in the cylindrical interference fit characteristic. On this basis, we have found that the major factor is the mean height of the asperities. This factor must be integrated into the definition of the tightening. We propose the peak to peak tightening definition as the right parameter permitting the calculation of the pressure with the standard equation (1). We think that the roughness contributes to the fit strength, and it is advisable to use economical manufacturing processes as turning or boring to produce the fit surfaces, as opposed to polishing or grinding methods that are much more expensive.

References

Bay, N., Wahnheim, T., 1976. Real area of contact and friction stress at high pressure sliding contact. Wear 38, 201–209.

Boulanger, J., 1992. The 'motifs' method: an interesting complement to the ISO parameters for some functional problems. Int. J. Mach. Tools Manufact. 32 (1/2), 203–209.

Bowden, F.P., Tabor, D., 1958. The Friction and Lubrication of Solids. Clarendon Press, Oxford.

Childs, T.H.C., 1977. The persistence of roughness between surfaces in static contact. Proc. R. Soc. Lond. A 353, 35–53.

Fontaine, J.F., Siala, I.E., 1998. Form defect influence on the shrinkage fit characteristics. Eur. J. Mech. A/ Solids 17 (1), 107–119.

Ike, H., Makinouchi, A., 1990. Effect of lateral tension and compression on plane strain fattering processes of surface asperities lying over a plastically deformable bulk. Wear 140, 17–38.

Moore, A.J.W., 1948. Proc. R. Soc. Lond. A 195, 213–243.

Nicolet, G., Trottet, J., 1971. Elément de machines, Lausanne.

NF E22-620, 1984. Assemblage frettés sur portée cylindrique: Fonction, réalisation, calcul., AFNOR, Paris la défense.

NF E22-621, 1980. Assemblage frettés, dimensions, tolérances et états de surface pour assemblages usuels, AFNOR, Paris la défense.

Sutcliffe, M.P.F., 1988. Surface asperity deformation in metal forming processes. Int. J. Mech. Sci. 30, 847–868.

Willamson, J.B.P., Hunt, 1972. Asperity persistence and the real area of contact between rough surfaces. Proc. R. Soc. Lond. A 327, 147–157.

Yang, G.M., 1998. Influence de l'état de surface sur les caractéristiques d'un assemblage fretté. Thèse de doctorat ENSAM, France.